Multi-Timescale Nonlinear Robust Control for a Miniature Helicopter

Yunjun Xu

Abstract— **This paper proposes a new nonlinear control approach which is applied to a miniature aerobatic helicopter through a multi-timescale structure. To deal with inherent unstable internal dynamics, the translational, rotational, and flapping dynamics of the helicopter are organized into a three-timescale nonlinear model. The concepts of dynamic inversion and sliding manifold are combined together. Part of the uncertainties is explicitly taken into account in the nonlinear robust control design, and Monte Carlo simulations are used for validations under other sensor noises and model uncertainties.**

Index Terms— **Miniature helicopter, multi-timescale, nonlinear system, robust control, under-actuated system.**

I. INTRODUCTION

The evolution of the Unmanned Aerial Vehicle (UAV) is at a tremendous pace these days. However, in order to respond to a growing market's demand and operate in the US National Airspace System (NAS), UAVs require the Certificate of Authorization from the Federal Aviation Administration (FAA) [1], [2]. Typically, the practice in rotary wing UAV flight control is to linearize the aircraft dynamics about different trim conditions and use gain scheduled linear control techniques to control the helicopter during different flight conditions. Mismatches and uncertainties among these operating points are captured through different robust control methodologies such as H_∞ [4], [5], μ control [6], neural nets [7] or fuzzy logic [8]. However, aerodynamic forces acting on a rotary wing UAV changes dramatically when it operates between different flight conditions. To design a controller for operations in the full flight envelope, dynamic inversion, input-output feedback linearization or sliding mode control (SMC) is typically used [6], [9]-[11]. Because of the under-actuated nature, a pseudo inverse is normally experienced. Numerical errors can not be avoided and the induced internal dynamics instability may occur even with the help of singular value decomposition techniques. Two of the typical methodologies used to address this problem are timescale separation (TSS) [12], [13] and the State-Dependant Riccati Equation control (SDRE) [14]. In the SDRE approach, only the part of the system that is not able to be presented in the state dependant

coefficient (SDC) form needs to be inverted.

This paper is mainly concerned with the development of a general multiple-input-multiple-output (MIMO) nonlinear robust controller, which combined with the three-timescale structure (three resolvable problems) can be applied in a specific miniature helicopter control problem. Different from [12] and [13] where a two-timescale model is used and the flapping motion is assumed to be quasi-static, three timescales are used where the flapping motion is regarded as the fastest mode explicitly. In each timescale, a uniform nonlinear robust controller is designed with guaranteed stability and is robust with respect to explicitly considered parametric uncertainties and unmodeled dynamics. Unlike a typical SMC [15]-[19], there is no discontinuity function or non-ideal switch, which typically results in the chattering phenomenon [20], [21]. In the mean time, the controller is guaranteed to be insensitive to bounded parametric and functional uncertainties, which is better than a typical dynamic inversion approach.

The rest of the paper is organized as follows. First the Lyapunov stability based nonlinear robust control is derived and the existence and uniqueness of the feedback control gain are proved. Second, led by the analytical stability study, some characteristics of the proposed nonlinear control method are discussed. After that, the three-timescale miniature helicopter dynamics model is briefly listed. Then controllers are designed and validated through Monte Carlo simulations for each timescale. Finally, the overall simulation results are demonstrated and a conclusion is drawn.

II. NONLINEAR ROBUST TRACKING CONTROL

A. General Case

Let us consider a nonlinear system with a state function of

$$x_i^{(n_i)} = f_i(\boldsymbol{x}_1,...,\boldsymbol{x}_n,t) + \sum_{j=1}^{m} b_{ij}(\boldsymbol{x}_1,...,\boldsymbol{x}_n)u_j, \, i=1,...,n, \, j=1,...,m \quad (1)$$

and an output function of

$$y_i = h_i(\boldsymbol{x}_1,...,\boldsymbol{x}_n), \, i=1,...,p \quad (2)$$

where $\boldsymbol{x}_i = \left[x_i,...,x_i^{(n_i-1)}\right]^T \in \Re^{n_i}$ and $x_i^{(n_i-1)} \triangleq d^{n_i-1}x_i/dt^{n_i-1}$ are states with up to n_i-1 derivatives. $\boldsymbol{u} = [u_1,...,u_m]^T \in \Re^m$ is the control input and $\boldsymbol{B} = \left[b_{ij}(\boldsymbol{x}_1,...,\boldsymbol{x}_n)\right] \in \Re^{n \times m}$ is the input matrix. $\boldsymbol{f} = [f_1,...,f_n]^T \in \Re^n$ is the nonlinear state function. The relative degree for the output $\boldsymbol{y} = \boldsymbol{h} = [y_1,...,y_p]^T \in \Re^p$ is

$r = [r_1,...,r_p]^T \in \Re^p$. To avoid numerical errors in pseudo inverse associated with the proposed controller, $p \le m$ is required. The aim of the controller is capable of tracking the desired trajectory $y_{i,d}, i = 1,...,p$. The nominal model is

$$x_i^{(n_i)} = \hat{f}_i(x_1,...,x_n,t) + \sum_{j=1}^{m} \hat{b}_{ij}(x_1,...,x_n)u_j, \ i=1,...,n, \ j=1,...,m \quad (3)$$

and the nominal measured output is $y_i = \hat{h}_i(x_1,...,x_n)$, where $\wedge$ represents the predicted information, $\hat{f} = [\hat{f}_1,...,\hat{f}_n]^T \in \Re^n$ and $\hat{B} = \left[\hat{b}_{ij}(x_1,...,x_n)\right] \in \Re^{n \times m}$. The parametric uncertainties of the input matrix are bounded by $\left|\Delta_{ij}\right| \le D_{ij} < 1, \ i,j = 1,...,p$ as

$$(I + \Delta) = \left[L_B L_f^{r-1} h(x) \right]\left[L_{\hat{B}} L_{\hat{f}}^{r-1} \hat{h}(x) \right]^+, \Delta \in \Re^{p \times p} \quad (4)$$

where I is an identity matrix with the proper dimension. B and $\hat{B}$ are assumed to satisfy the matching condition. " L " and " $+$ " are used to denote the Lie derivative and the pseudo inverse respectively. The error between the predicted and actual state functions is bounded by

$$F_i = \left| -L_f^{r_i} h_i + L_f^{r_i} \hat{h}_i \right|, \ i = 1,...,p \quad (5)$$

The sliding manifold $s = [s_1,...,s_p]^T \in \Re^p$ is

$$s_i = \lambda_{-1,i}\int e_i dt + \sum_{k=0}^{r_i-2} \lambda_{k,i} e_i^{(k)} + e_i^{(r_i-1)}, i = 1,...,p \quad (6)$$

where $\lambda_{k,i} > 0, \ k = -1,...,r_i - 2$ can be any positive number and the error signal is defined to be $e_i = y_{i,d} - y_i, \ i = 1,...,p$.

Theorem 1: For a nonlinear system (1) with bounded parametric and functional uncertainties (5) and (6), the proposed MIMO feedback control scheme

$$u = \left[L_{\hat{B}} L_{\hat{f}}^{r-1} \hat{h}(x) \right]^+ \left[\frac{d^r y_d}{dt^r} - L_f^r \hat{h}(x) + \lambda_{-1} \cdot e + \sum_{k=0}^{r-2} \lambda_k \cdot e^{(k+1)} + k \cdot s \right] (7)$$

guarantees that the closed-loop system is globally asymptotically stable for tracking desired signal $y_{i,d}$. Note that element-wise multiplication $a \cdot b = [a_1 b_1,...,a_p b_p]^T$ is used. An explicit time varying feedback gain $k = [k_1,...,k_p]^T$ will be obtained from the stability proof below (Section II.B).

Unlike the SMC or boundary layer augmented SMC (BASMC), there is no discontinuous function (or switching function) involved in the proposed controller and therefore chattering is avoided. This property is crucial to the multi-timescale robust controller to be used in the miniature helicopter control problem.

Proof: Stability of the control law is ensured through the analysis of the Lyapunov function candidate $V = s^T s/2$, The derivative of the Lyapunov function is $\dot{V} = \sum_{i=1}^{p} v_i = \sum_{i=1}^{p} \dot{s}_i s_i$.

$$\dot{s} = -L_f^r h(x) + L_f^r \hat{h}(x) - k \cdot s$$
$$- \Delta \left[\frac{d^r y_d}{dt^r} - L_f^r \hat{h}(x) + \lambda_{-1} \cdot e + \sum_{k=0}^{r-2} \lambda_k \cdot e^{(k+1)} + k \cdot s \right] \quad (8)$$

Using parametric uncertainty and functional uncertainty bounds, when $s_i(t) \ne 0$

$$\dot{s} \le F - (I-D)k \cdot s + D\left| \frac{d^r y_d}{dt^r} - L_f^r \hat{h}(x) + \lambda_{-1} \cdot e + \sum_{k=0}^{r-2} \lambda_k \cdot e^{(k+1)} \right| = -\eta \cdot s \quad (9)$$

Therefore the gain is calculated by

$$F + D\left| \frac{d^r y_d}{dt^r} - L_f^r \hat{h}(x) + \lambda_{-1} \cdot e + \sum_{k=0}^{r-2} \lambda_k \cdot e^{(k+1)} \right| + \eta \cdot s = (I-D)k \cdot s \quad (10)$$

When $s_i(t) = 0$, we have $v_i = 0$ and $\dot{v}_i = 0$. Therefore the reaching and sliding on the sliding manifold $s_i = 0$ are guaranteed. Here, v_i is lower bounded by zero, and $\dot{v}_i$ is negative semi-definite. Because $\dot{v}_i \le 0$ and $v_i(t) \le v_i(0)$, the output and output tracking errors are bounded. Thus, $\dot{s}_i$ and s_i are also bounded. For the continuous functions $\dot{s}_i$ and $\ddot{s}_i$, $\ddot{v}_i = s_i \ddot{s}_i + \dot{s}_i \dot{s}_i$ are also bounded, which means $\dot{v}_i(x_1,...,x_n,t)$ is uniformly continuous over time. According to the Barbalat's Lemma [22], $\dot{v}(x,t) \to 0$ as $t \to \infty$ and thus the controlled system is asymptotically stable.

B. Existence of a Solution to k

Lemma 1: There exists a unique positive solution for the control gain k that satisfies (10) for any positive numbers λ and η. *Proof:*

For $\forall s_i > 0$, the Lyapunov stability requires

$$F_i + \sum_{j=1}^{p} D_{ij} \mid y_{j,d}^{r_j} - L_f^{r_j} \hat{h}_j + \lambda_{-1,j} e_j + \sum_{k=0}^{r_j-2} \lambda_{k,j} e_j^{(k+1)} \mid + \eta_i s_i = k_i s_i - \sum_{j=1}^{p} D_{ij} \mid k_j s_j \mid \quad (11)$$

while for $\forall s_i < 0$, the Lyapunov stability requires

$$F_i + \sum_{j=1}^{p} D_{ij} \mid y_{j,d}^{r_j} - L_f^{r_j} \hat{h}_j + \lambda_{-1,j} e_j + \sum_{k=0}^{r_j-2} \lambda_{k,j} e_j^{(k+1)} \mid - \eta_i s_i = -k_i s_i - \sum_{j=1}^{p} D_{ij} \mid k_j s_j \mid \quad (12)$$

Case 1: $s_i > 0$ or $s_i < 0, \ \forall i \in [1,...,p]$,

Under this case, both (11) and (12) can be written as

$$F_i + \sum_{j=1}^{p} D_{ij} \mid y_{j,d}^{r_j} - L_f^{r_j} \hat{h}_j + \lambda_{-1,j} e_j + \sum_{k=0}^{r_j-2} \lambda_{k,j} e_j^{(k+1)} \mid + \mid \eta_i s_i \mid = \mid k_i s_i \mid - \sum_{j=1}^{p} D_{ij} \mid k_j s_j \mid \quad (13)$$

Let us define $\varsigma_i = \mid k_i s_i \mid > 0$ and $\zeta = [\zeta_1,...,\zeta_1] \in \Re^p$. Equation (13) can be written in a vector form as $\zeta = \varsigma - D\varsigma = (I - D)\varsigma$, where

$$\zeta_i = F_i + \sum_{j=1}^{p} D_{ij} \mid y_{j,d}^{r_j} - L_f^{r_j} \hat{h}_j + \lambda_{-1,j} e_j + \sum_{k=0}^{r_j-2} \lambda_{k,j} e_j^{(k+1)} \mid + \mid \eta_i s_i \mid \quad (14)$$

Because of the uncertainty matching function [22], the maximum eigenvalue of matrix D is less than 1. According to the Perron–Frobenius theorem, if $\zeta > 0$, and the maximum eigenvalue of matrix D is less than 1. Thus there exists a unique solution of ς and $\varsigma > 0$. The unique and positive k can be found by $k_i = \mid \varsigma_i / s_i \mid, s_i \ne 0$. In case of $s_i \to 0$, the magnitude of $k_i s_i$ ($\varsigma_i = \mid k_i s_i \mid$) instead of k_i will be calculated because the proposed controller (8) only uses $k_i s_i$.

Case 2: $s_l > 0$, $s_q < 0$, $\forall l,q \in [1,...,p]$ and $q \ne l$

Let us define $\varsigma_l = k_l s_l$ for $s_l > 0$ and $\varsigma_q = -k_q s_q$ for $s_q < 0$. Equations (11) and (12) can be simplified as

$$F_l + \sum_{j=1}^{p} D_{lj} \left| y_{j,d}^{r_j} - L_f^{r_j} \hat{h}_j + \lambda_{-1,j} e_j + \sum_{k=0}^{r_j-2} \lambda_{k,j} e_j^{(k+1)} \right| + \eta_l s_l = k_l s_l - \sum_{j=1}^{p} D_{lj} \left| k_j s_j \right| \quad (15)$$

and

$$F_q + \sum_{j=1}^{p} D_{qj} \left| y_{j,d}^{r_j} - L_f^{r_j} \hat{h}_j + \lambda_{-1,j} e_j + \sum_{k=0}^{r_j-2} \lambda_{k,j} e_j^{(k+1)} \right| - \eta_q s_q = -k_n s_n - \sum_{j=1}^{p} D_{nj} \left| k_j s_j \right| \quad (16)$$

The left side of both Eqs. (15) and (16) are positive. Based on the same derivation as shown in Case 1, there exists a unique and positive solution for ς, from which a unique k can be calculated explicitly.

III. CHARACTERISTICS OF THE CONTROLLER

A. Chattering Free

As a typical dynamic inversion approach, the proposed nonlinear robust control removes the discontinuous function.

B. Saturation Protection

It is often true that saturation happens in the initial stage of a tracking problem and the corresponding initial gain is large. Let us use the second order system as an example. The control feedback gain k (in SMC) is calculated by

$$F + D \left| \ddot{y}_d - L_f^2 \hat{h}(x) + \lambda_{-1} \cdot e + \lambda_0 \cdot \dot{e} \right| + \eta = (I - D) k \quad (17)$$

and is not affected by the sliding manifold. We can simplify the control gain calculation as $k = (I-D)^{-1} p + (I-D)^{-1} \eta$ where p is defined as $F + D \left| \ddot{y}_d - L_f^2 \hat{h}(x) + \lambda_{-1} \cdot e + \lambda_0 \cdot \dot{e} \right|$. It can be seen that the control feedback gain k will not reflect the slow transient effects due to the saturation. However, the solution of k in the proposed controller is found as

$$(I-D)^{-1} p./s + (I-D)^{-1} \eta = k \quad (18)$$

where $p./s = [p_1/s_1, ..., p_m/s_m]^T$.

IV. MINIATURE HELICOPTER DYNAMICS IN THREE TIMESCALES

Different from [12], [13], three timescales are used. Separations are made among the fast mode (i.e. flapping dynamics), the middle mode (i.e. attitude dynamics), and the slow mode (i.e. translational dynamics). The idea is to control the flapping dynamics at the fastest rate (1 kHz). The control inputs $\mathbf{u}_f$ for the fast mode are the main rotor collective δ_{col}, longitudinal cyclic δ_{lon} and lateral cyclic δ_{lat}. The pedal δ_{ped}, a_1 and b_1 are used as the control vector $\mathbf{u}_m$ for the middle mode (100 Hz) to track the desired Euler angles $[\phi_d, \theta_d, \psi_d]^T$. In the slow mode, two of the Euler angles, $[\phi, \theta]^T$, and the main engine thrust T_{mr} will be regarded as the control $\mathbf{u}_s$ for controlling the body velocity. In the slow mode (10 Hz), the roll, pitch and yaw rates, and δ_{ped}, a_1 and b_1 are all in the average sense (within the sampling period of the slow mode). Due to the page limit,

detailed information and nomenclature of the miniature helicopter model can be found in [24] and will not be listed here. Here, to simplify the control design, the dynamics model has been re-organized in a much clearer way.

A. Fast Mode

In this paper, the flapping dynamics is considered as the fast model

$$\begin{bmatrix} \dot{a}_1 \\ \dot{b}_1 \end{bmatrix} = \begin{bmatrix} -q - \dfrac{a_1}{\tau_e} + \left(\dfrac{16\mu^2 K_\mu}{8|\mu|+a\sigma} sign(\mu) \right) \dfrac{w_a}{\tau_e \Omega R} - 2K_\mu \lambda_0 \dfrac{u_a}{\tau_e \Omega R} \\ -p - \dfrac{b_1}{\tau_e} - \dfrac{2K_\mu \lambda_0}{\tau_e} \dfrac{v_a}{\Omega R} \end{bmatrix}$$

$$+ \begin{bmatrix} \dfrac{8K_\mu}{3\tau_e} \dfrac{u_a}{\Omega R} & A_{\delta_{lon}}^{norm} \left(\dfrac{\Omega}{\Omega_{norm}} \right)^2 & 0 \\ \dfrac{8K_\mu}{3\tau_e} \dfrac{v_a}{\Omega R} & 0 & \dfrac{B_{\delta_{lat}}^{norm}}{\tau_e} \left(\dfrac{\Omega}{\Omega_{norm}} \right)^2 \end{bmatrix} \begin{bmatrix} \delta_{col} \\ \delta_{lon} \\ \delta_{lat} \end{bmatrix} \quad (19)$$

where the state is $\mathbf{x}_f = [a_1, b_1]^T$, the advance ratio is $\mu = \sqrt{u_a^2 + v_a^2}/(\Omega R)$, and the control input vector is $\mathbf{u}_f = [\delta_{col}, \delta_{lon}, \delta_{lat}]^T$. Also the relative velocities of the helicopter with respect to the wind are $u_a = u - u_w$, $v_a = v - v_w$, and $w_a = w - w_w$.

B. Middle Mode

The middle mode (attitude dynamics) is governed by

$$\begin{bmatrix} \dot{\phi} \\ \dot{\theta} \\ \dot{\psi} \\ \dot{p} \\ \dot{q} \\ \dot{r} \end{bmatrix} = \begin{bmatrix} p + q\sin\phi\tan\theta + r\cos\phi\tan\theta \\ q\cos\phi - r\sin\phi \\ q\sin\phi\sec\theta + r\cos\phi\sec\theta \\ qr(I_{yy}-I_{zz})/I_{xx} + (L_{vf}+L_{tr})/I_{xx} \\ pr(I_{zz}-I_{xx})/I_{yy} + M_{ht}/I_{yy} \\ pq(I_{xx}-I_{yy})/I_{zz} + (N_{vf}+N_{tr}-Q_e)/I_{zz} \end{bmatrix}$$

$$+ \begin{bmatrix} 0 \\ 0 \\ 0 \\ h_{tr} m Y_{\delta_r}^{tr}/I_{zz}\delta_{ped} + \left[K_\beta + T_{mr}(\Omega)h_{mr} \right]/I_{xx} b_1 \\ \left[K_\beta + T_{mr}(\Omega)h_{mr} \right]/I_{yy} a_1 \\ -m Y_v^{tr} l_{tr}/I_{xx}\delta_{ped} \end{bmatrix} \quad (20)$$

where the state vector is $\mathbf{x}_m = [\phi, \theta, \psi, p, q, r]^T$ and the control input is $\left[\delta_{ped}, a_1, b_1 \right]^T$. The detailed information of the moments and forces can be found in [24].

C. Slow Mode

In the slow mode (translational motion), the state and the control vectors are defined as $\mathbf{x}_s = [u, v, w]^T$ and $\mathbf{u}_s = [T_{mr}, a_1, b_1]^T$. The governing equation is

$$\begin{bmatrix} \dot{u} \\ \dot{v} \\ \dot{w} \end{bmatrix} = \begin{bmatrix} v\bar{r} - w\bar{q} + X_{fus}/m \\ w\bar{p} - u\bar{r} + [Y_{fus} + \bar{Y}_{vf} + \bar{Y}_{tr}]/m + Y_\delta^{tr}\bar{\delta}_{ped} \\ u\bar{q} - v\bar{p} + Z_{fus}/m \end{bmatrix}$$
$$+ \begin{bmatrix} -g\sin\theta + (-a_1/m)T_{mr} \\ g\sin\phi\cos\theta + (b_1/m)T_{mr} \\ g\cos\phi\cos\theta + (-1/m)T_{mr} \end{bmatrix} \quad (21)$$

where symbols with over-bars denote variables that are evaluated using the average values from the middle mode. The forces generated by the fuselage are

$$X_{fus} = -0.5\rho S_x^{fus} u_a V_\infty \quad (22)$$

$$Y_{fus} = -0.5\rho S_y^{fus} v_a V_\infty \quad (23)$$

and

$$Z_{fus} = -0.5\rho S_z^{fus}(w_a + V_{imr})V_\infty \quad (24)$$

where $V_\infty = \sqrt{u_a^2 + v_a^2 + (w_a + V_{imr})^2}$.

V. FAST MODE CONTROL AND MONTE CARLO VALIDATION

The fast mode controller is designed to track reference lateral and longitudinal flapping angles $a_{1,d}$ and $b_{1,d}$ respectively. The settling time needs to be less than the sampling period of the middle mode (0.01s) and the steady state error are assumed to be within 5% (uncertainty bounds considered by the middle mode). Let us denote the fast mode to be $\dot{x}_f = f_f(x) + B_f u_f$ and $y_f = x_f$, where subscript f designates the fast mode. The uncertainties in the fast mode state function are modeled as $|\hat{f}_{f,i} - f_{f,i}| \le F_{f,i}$, $i = 1,2$ and those of the input matrix are

$$B_f = (I + \varDelta_f)\hat{B}_f, \quad |\Delta_{f,ij}| \le D_{f,ij} < 1, \quad i = 1,2, j = 1,2 \quad (25)$$

where " $\wedge$ " represents the nominal modes.

Since the relative degree for the fast mode is one, the nonlinear robust controller can be simplified as

$$u_f = \hat{B}_f^+\left[\dot{y}_d - \hat{f}_f + k_f \cdot s_f\right] \quad (26)$$

without the integral gain, where $s_f = e_f = y_{f,d} - y_f$. To satisfy the asymptotical stability requirement under bounded uncertainties, the control parameter k_f needs to satisfy

$$F_{f,i} + \sum_{j=1}^2 D_{f,ij}\left|\dot{y}_{f,j,d} - \hat{f}_{f,j}\right| + \eta_{f,i}s_{f,i} = k_{f,i}s_{f,i} - \sum_{j=1}^2 D_{f,ij}k_{f,i}s_{f,i} \quad (27)$$

where $\eta_{f,i} > 0, \ i = 1,2$.

The following random noise and uncertainties (all assumed to be Gaussian) are considered in the Monte Carlo simulation for the fast mode. The wind model is scaled (10%) from the one designed for conventional large aircraft [25]. The airspeed indicator and attitude sensors are assumed to have 2% noise. The estimated states a_1 and b_1 are assumed to have 1% noise. There are 5% uncertainties in the helicopter parameters K_μ, τ_e, Ω_{mr}, c_{mr}, a_{mr}, $A_{\delta_{lon}}^{norm}$, and $B_{\delta_{lat}}^{norm}$, whereas R_{mr} and λ_0 have 0.5% and 1% noises

respectively. The control u_f has a noise with a zero mean and 1° standard deviation. With 12,500 Monte Carlo simulations, the success rate was 99.97%. The mean and variance of the settling time (a_1) are 0.0040s and 0.0039s, whereas those of b_1 are 0.0045s and 0.0034s. The mean and variance of the steady state error (a_1) are 0.6602% and 0.2411%, whereas those of b_1 are 1.2286% and 1.6420%.

VI. MIDDLE MODE CONTROL AND MONTE CARLO VALIDATION

Let us rewrite the fast mode to be $x_m = f_m(x) + B_m u_m$. The output for the middle mode is $y_m = h_m = [\phi, \theta, \psi]^T$, and the relative degree is two. To take into account modeling uncertainties and achieve asymptotic stability, the following controller is used

$$u_m = \left[L_{\hat{B}_m}L_{\hat{f}_m}h_m(x)\right]^{-1}\left[\ddot{y}_d - L_{\hat{f}_m}^2 h_m(x) + 2e_m + \dot{e}_m + k_m \cdot s_m\right](28)$$

where $e_m = y_{d,m} - y_m$. The " $\wedge$ " denotes a predicted model.

In order to reduce the steady state error and settling time, an integral gain is used in the sliding surface

$$s = \left[s_i\right]_{i=1,\dots,3} = \left[\int e_i dt + \sum_{k=0}^1 \beta_k \frac{d^k e_i}{dt^k}\right]_{i=1,\dots,3} \quad (29)$$

The uncertainties in the state equation and input matrix are modeled as

$$\left|-L_f^2 h(x) + L_{\hat{f}}^2 h(x)\right| = \left|\frac{\partial L_f^1 h(x)}{\partial x}(\hat{f} - f)\right| = F \in \Re^{3\times 1} \quad (30)$$

and

$$\left(\partial L_f^{r-1}h(\mathbf{x})/\partial x\right)B = (I + \varDelta)\left[\left(\partial L_{\hat{f}}^{r-1}h(\mathbf{x})/\partial x\right)\hat{B}\right] \quad (31)$$

To obtain asymptotic stability, control parameters k_m need to satisfy

$$F_m + D_m\left|\frac{d^2 y_d}{dt^2} - L_{\hat{f}_m}^2 h_m(x_m) + \sum_{k=0}^{r-1}\beta_k\frac{d^k e_m}{dt^k}\right| + \eta_m \cdot s_m = (I - D_m)k_m \cdot s_m \quad (32)$$

The noise associated with the helicopter parameters ($I_{xx}, I_{yy}, I_{zz}, h_{tr}, K_\beta, h_{mr}, l_{tr}$) are modeled to have zero means and 5% of the nominal value in the standard deviation. Also, 0.5% noise is assumed in the helicopter mass and 10% uncertainties are modeled in $Y_{\delta_r}^{tr}$, V_{itr} and V_{imr}. Coming from the fast model, 5% noise is assumed in the flapping dynamics (a_1 and b_1), and the pedal input δ_{ped}.

The success rate is 99.48% with 13,000 Monte Carlo simulations. The driving factors associated with the middle mode performance are the mass m and the attitude sensor precision. The mean values of the settling time are 0.0569s (ϕ) and 0.0570s (θ). The variances of the settling time are 0.0002s and 0.0003s. The mean values of the steady state error are 2.5854% (ϕ) and 2.1767% (θ). The variances are 8.9045% and 10.0823% separately.

VII. Slow Mode Control and Monte Carlo Validation

At this level, the Euler angles will be used to drive the translational velocity to desired values. The state vector in the slow mode is $x_s = [u,v,w]^T$ and the control variables are $[\phi,\theta,T_{mr}]^T$. Now, the system dynamics can be written as $\dot{x}_s = f_s + B_s u_s$ where $u_s = [\varsigma_1,\varsigma_2,\varsigma_3]^T$. $\bar{x}_m = [\bar{p},\bar{q},\bar{r}]^T$ and $\bar{u}_m = [\bar{a}_1,\bar{b}_1,\bar{\delta}_{ped}]^T$ represent the average state and control from the middle mode.

The control designed for the slow mode involves two steps (1) a nonlinear robust control law u_s to track desired body velocity $[u_d,v_d,w_d]^T$ and (2) using the control commands u_s to solve for desired Euler angles and thrust levels through a zero finding algorithm.

Since the output in the slow mode is $y_s = x_s$, the full state feedback controller is designed for step 1. The uncertainty model for the slow mode is $|\hat{f}_s - f_s| \le F_s$ and

$$B_s = (I + \Delta_s)\hat{B}_s, \quad (\Delta_s)_{ij} \le (D_s)_{ij} < 1 \quad (33)$$

These uncertainties may come from (1) sensor noise, (2) average value of the middle mode state and control variables, (3) steady state error of the Euler angle, and (4) zero finding algorithm error.

Since the relative degree is one in this case, the nonlinear robust control can be simplified as $u_s = \hat{B}_s^{-1}[\dot{x}_{s,d} - \hat{f}_s + k_s \cdot s_s]$, where $s_s = e_s = x_{s,d} - x_s$ and the control parameter needs to satisfy $k_s \cdot s_s = (I_s - D_s)^{-1}(F_s + D_s|\dot{x}_{s,d} - \hat{f}_s| + \eta_s \cdot s_s)$, where $\eta_s > 0$.

The true control variables $[\phi,\theta,T_{mr}]^T$ can be found as following. First, the controls found and $[\phi,\theta,T_{mr}]^T$ have the following relations.

$$\begin{bmatrix} \varsigma_1 + (T_{mr}/m)\bar{a}_1 \\ \varsigma_2 - (T_{mr}/m)\bar{b}_1 \\ \varsigma_3 + T_{mr}/m \end{bmatrix} = \begin{bmatrix} -g\sin\theta \\ g\sin\phi\cos\theta \\ g\cos\phi\cos\theta \end{bmatrix} \quad (34)$$

The magnitude of both sides is equal as

$$(\varsigma_1 + \bar{a}_1 T_{mr}/m)^2 + (\varsigma_2 - \bar{b}_1 T_{mr}/m)^2 + (\varsigma_3 + T_{mr}/m)^2 = g^2 \quad (35)$$

and the thrust can be found as

$$T_{mr} = \left(-\xi_2 \pm \sqrt{\xi_2^2 - 4\xi_1\xi_3}\right)/(2\xi_1) \quad (36)$$

where

$$\xi_1 = \left[(\bar{a}_1/m)^2 + (\bar{b}_1/m)^2 + (1/m)^2\right]T_{mr}^2 \quad (37)$$

$$\xi_2 = \left(2\varsigma_1\bar{a}_1/m - 2\varsigma_2\bar{b}_1/m + 2\varsigma_3/m\right)T_{mr} \quad (38)$$

and $\xi_3 = \varsigma_1^2 + \varsigma_2^2 + \varsigma_3^2 - g^2$.

To guarantee a valid solution for the main rotor thrust, it is required to have $\xi_3 = \varsigma_1^2 + \varsigma_2^2 + \varsigma_3^2 - g^2 \le 0$ and the velocity

command will be shaped to avoid rapid changes.

The Euler angles (ϕ and θ) can be calculated from Eq. (34) as

$$\sin\theta = -\left[\varsigma_1 + (T_{mr}/m)\bar{a}_1\right]/g \quad (39)$$

and

$$\tan\phi = \left[\varsigma_2 - (T_{mr}/m)\bar{b}\right]/\left[\varsigma_3 + T_{mr}/m\right] \quad (40)$$

The Euler angle controlled by the middle mode has 10% steady state error. In addition to the uncertainties and noises already mentioned in the fast and middle modes, the gravity coefficient g and corresponding density ρ are assumed to have 0.5% uncertainties. η_w has a zero-mean noise with a 1% in the standard deviation. In the 10,500 Monte Carlo runs, the success rate is 97.10%. The mean values for the settling time in velocity tracking (u, v, and w) are 1.9994s, 1.9937s, and 0.4059s respectively, whereas the variances are 0.0111s, 0.0068s, and 0.0196s. The mean values of the steady state errors in three directions are 0.0141 %, 0.0074%, and 0.0602%. The corresponding variances are 3.8931%, 1.7115%, and 17.0253%.

VIII. Simulation Results

The miniature helicopter is assumed to fly at an altitude of 300m. Initially, the helicopter is in a hover mode with a zero velocity. As shown in Fig. 1, the helicopter is able to track the desired velocity ($u_d = 1\,m/s$, $v_d = 1\,m/s$, and $w_d = 1\,m/s$) for the first five seconds and go back to hover mode for the later five seconds without any chatter.
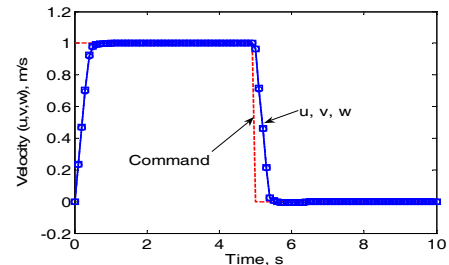

Fig. 1 Velocity tracking in u, v, and w

The main rotor collective and the tail rotor pedal input are shown in Fig. 2, where the pedal input has more oscillations in the slow mode scale. The longitudinal cyclic and lateral cyclic of the main rotor are shown in Fig. 3. The main rotor thrust and engine speed performance is show in Fig. 4.
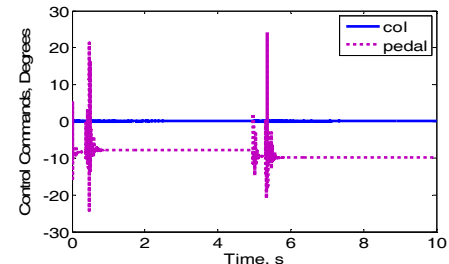

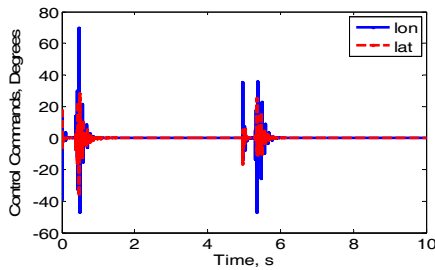Fig. 2 Main rotor collective and the pedal input.

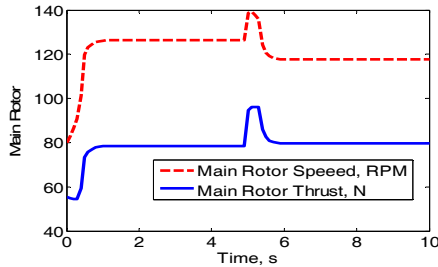Fig. 3 Main rotor longitudinal and lateral cyclic.

Fig. 4 Main engine speed and main rotor thrust.

IX. CONCLUSION

A nonlinear robust control algorithm is proposed here which could enable a miniature helicopter to operate in the full flight envelop. In addition, the controller is valid for general n^{th} order MIMO systems with coupled uncertainties in state and input functions and parameters. The miniature helicopter is controlled through a three-timescale (flapping, rotational, and translational models) nonlinear robust controller. The advantage of the proposed controller is to have a finite time convergence and guaranteed settling time, which is preferred for the multi-timescale control structure. The unique solution of the control feedback gain is guaranteed. Monte Carlo simulations are conducted for the validation of the proposed controller for each of the three modes.

REFERENCES

[1] RTCA SC-186, "Application of airborne conflict management: detection, prevention, & resolution", *RTCA DO-263,* Dec. 14, 2000, Washington, DC, RTCA, Inc.

[2] K. Krishnamurthy, and D. J. Wing, et al., "Autonomous aircraft operations using RTCA guidelines for airborne conflict management", *Digital Avionics Systems Conference*, Oct. 12 2003.

[3] http://www.nasa.gov/centers/dryden/news/NewsReleases/2003/03-20.html, last access: July 2007.

[4] M. La Civita, G. Papageorgiou, W. C. Messner, and T. Kanade, "Design and flight testing a high-bandwidth H_∞ loop shaping controller for a robotic helicopter," *Proceedings of the AIAA Guid., Navigation, and Control Conf.*, AIAA, Reston, VA, 2000.

[5] M. D. Takahashi, "H_∞ helicopter flight control law design with and without rotor state feedback," *J. Guid. Control Dyn.,* vol. 17, no. 6, pp. 1245-1251, Nov.-Dec. 1994.

[6] J. Reiner, G. J. Balas, and W. L. Garrard, "Flight control design using robust dynamic inversion and time-scale separation," *Automatica*, Vol. 32, Issue 11, 1996, pp. 1493-1504.

[7] N. Hovakimyan, N. Kim, A. J. Calise, and J. V. R., Prasad, "Adaptive output feedback for high-bandwidth control of an unmanned helicopter," *AIAA Guid., Navigation, and Control Conference*, Montreal, Quebec, Canada, Aug. 2001

[8] H. Shim, T. J. Koo, F. Hoffmann, and S. Sastry, "A comprehensive study on control design of autonomous helicopter," *Proceedings of the IEEE Conference on Decision and Control*, Vol. 4, Piscataway, NJ, 1998, pp. 3653-3658.

[9] N. Paulino, C. Silvestre, and R. Cunha, "Affine parameter-dependent preview control for rotorcraft terrain following flight," *J. Guid. Control Dyn.,* vol. 29, no. 6, pp. 1350-1359, Nov.-Dec. 2006.

[10] N. A. Sahani and J. F. Horn, "Adaptive model inversion control of a helicopter with structural load limiting," *J. Guid. Control Dyn.,* vol. 29, no. 2, pp. 411-420, Mar.-Apr. 2006.

[11] D. J. McGeoch and E. W. McGookin, "MIMO sliding mode attitude command flight control system for A helicopter," *AIAA Guid., Navigation, and Control Conf. and Exhibit*, San Francisco, California, Aug. 2005, #AIAA 2005-6350.

[12] G. Avanzini, and G. Matteis, "Two-timescale inverse simulation of a helicopter model," *J. Guid. Control Dyn.,* vol. 24, no. 2, pp. 330-339, Mar.-Apr. 2001.

[13] S. Oh, J. C. Ryu, and S. K. Agrawal, "Dynamics and control of a helicopter carrying a payload using a cable-suspended robot," *J. Mechanical Design*, Vol. 128, Sept. 2006, pp. 1113-1121.

[14] A. Bogdanov, and E. Wan, "State-dependent riccati equation control for small autonomous helicopters," *J. Guid. Control Dyn.,* vol. 30, no. 1, pp. 47-60, Jan.-Feb. 2007.

[15] V. I. Utkin, "Variable structure systems with sliding modes," *IEEE Trans. Autom. Control*, vol. 22, no. 2, pp. 212-222, Apr. 1977.

[16] G. Bartolini, E. Punta, and T. Zolezzi, "Simplex methods for nonlinear uncertain sliding-mode control," *IEEE Trans. Autom. Control*, vol. 49, no. 6, pp. 922-933, Jun. 2004.

[17] J. Y. Hung, W. Gao, and J. C. Hung, "Variable structure control: a survey," *IEEE Trans. Ind. Electron.*, vol. 40, no. 1, pp. 2-22, Feb. 1993.

[18] A. S. Lewis and A. Sinha, "Sliding mode control of mechanical systems with bounded disturbances via output feedback," *J. Guid. Control Dyn.*, vol. 22, no. 2, pp. 235-240, Mar.-Apr. 1999

[19] S. K. Mudge and R. J. Patton, "Enhanced assessment of robustness for an aircraft's sliding mode controller," *J. Guid. Control Dyn.*, vol. 11, no. 6, pp. 500-507, Nov.–Dec. 1988

[20] Y. Xu and N. G. Fitz-coy, "Generalized relative dynamics and control in formation flying system," In *Proc. 26th Annu. AAS Guid. and Control Conf.*, Breckenridge, Colorado, Feb. 2003, Paper AAS 03-011.

[21] Y. Xu and N. G. Fitz-coy, "Genetic algorithm based sliding mode control in the leader/follower satellites pair maintenance," In *Proc. 2003 AAS/AIAA Astrodynamics Specialist Conf.,* Big Sky, Montana, Aug. 2003, Paper AAS 03-648.

[22] J. E. Slotine and W. Li, *Applied Nonlinear Control*. New Jersey: Prentice Hall, 1990, pp. 267-307.

[23] G. Bartolini, A. Ferrara, E. Usai, and V. I. Utkin, "On multi-input chattering-free second order sliding mode control," *IEEE Trans. Autom. Control*, vol. 45, no. 9, pp. 1711-1717, Sep. 2000.

[24] V. Gavrilets, B. Mettler, and E. Feron, "Dynamic model for a miniature aerobatic helicopter," *Department of Aeronautics and Astronautics*, MIT, Cambridge, USA.

[25] L. N. Lacey, "Criteria for approval of category III weather minima for takeoff, landing, and rollout," *AC 120-28D*, Federal Aviation Administration, July 13, 1999.